Article ID: 1003－6326(2004)03－0491－05

Modeling of microstructural evolution and flow stress of aluminium alloy during thermomechanical process①

SHEN Jian(沈 健)[1], G. Gottstein[2]
(1. General Research Institute for Nonferrous Metals, Beijing 100088, China;
2. Institut für Metallkunde und Metallphysik, RWTH-Aachen, Germany)

Abstract: The evolution of microstructural variables, including the densities of mobile dislocation, immobile dislocation at the cell interiors, immobile dislocation in the cell walls, as well as total dislocation density, of an Al-Mg-Si aluminium alloy during thermomechanical processing were simulated based on a three-internal-variables-model (3IVM) involving dislocation climb and interaction. Optimization was carried out to fit the calculated stress—strain curves to the experimental data of the Al-Mg-Si alloy with minimum mean deviation. Precipitations were taken into consideration of modeling. The stress—strain curves predicted by the kinetic equations of state in the 3IVM have a good agreement with the experimental data.

Key words: aluminium alloy; microstructure evolution; dislocation; modeling
CLC number: TG 146.2; TG 111.7 **Document code:** A

1 INTRODUCTION

Modeling of materials processing has been one of the most significant research fields in materials science and technology over the world in recent years, whilst modeling of microstructure evolution of advanced materials during deformation and recrystallization processes, which is necessary in the prediction of as-deformed microstructure and in optimization and controlling of the accordingly potential mechanical properties of the finished products, is one of the most interest topics. Basic understanding of computer modeling of testa- and microstructures evolution is a direct element in the precise microstructure and property prediction and control of advanced materials, where modeling based on interaction of dislocation is very important. Unfortunately, as indicated by Morris from UC Berkeley[1], this is still somewhat less integrated so far.

A large number of investigations have been carried out to simulate the evolution of flow stresses and microstructural features during hot working processes of many kinds of materials[2-8], such as subgrain size, dislocation density, misorientation among subgrains, etc. Flow stress and recrystallization behaviors of aluminum-magnesium alloy during hot rolling process were simulated and predicted by Sellars and his coworkers[2,9], where the variation of the subgrain size, dislocation density in the interior of subgrains and the misorientation between neighboring subgrains during steady state deformation were taken into consideration. The microstructure development under plastic deformation up to large strains was modelled by Seefeldt and Klimanek[8] by means of a four-component reaction kinetic for the density of mobile and immobile dislocations and disclinations. A relationship between the density of sessile disclinations and the flow stress was proposed using a Hall-Petch type relation for subgrain-size strengthening. An method to the modeling of work hardening during plastic deformation of pure FCC metals was proposed by Marthinsen and Nes[3], which is based on a statistical approach to the problem of athermal storage of dislocations. By combining the solution for the dislocation storage problem with the models for dynamic recovery of network dislocations and sub-boundary structures, a general internal state variable description was obtained. Effects due to the elements in solid solution and the presence of non-deformable precipitate particles were also included in the model, named ALFLOW, proposed by the authors. Semi-empirical microstructural models based on dislocation climb and interaction between dislocations were implemented into FEM programs by Brand et al[4] and Roters et al[5,6] to simulate microstructure evolution at imposed starting conditions of microstructure during multi-stage forging and multi-pass hot rolling operations.

The evolution of densities of mobile dislocations, immobile dislocations in the cell interiors and immobile dislocations in the cell walls for an Al-Mg-Si alloy

① **Foundation item:** Project(59701007) supported by the National Natural Science Foundation of China; Project(59911130885) supported by the International Coorperating Research Program of the National Natural Science Foundation of China
Received date: 2003－09－25; **Accepted date:** 2003－12－29
Correspondence: SHEN Jian, Professor, PhD; Tel: +86-10-82241261; E-mail: jshen@mail.grinm.com.cn

during hot compression was simulated in the present work by a three internal variables model of dislocations(3IVM) proposed by Roters et al[5, 6, 10]. The variation of flow stresses of the alloy predicted by modelling was analyzed and compared with the experimental data. Only climb of dislocation are taken into consideration in dynamic recovery process at elevated temperatures and consideration to cross slip of screw segments is limited.

2 THREE INTERNAL VARIABLES MODEL OF DISLOCATIONS(3IVM)

In dynamic recovery process, an inhomogeneous cellular dislocation arrangement composed of cell walls with high dislocation density develops in most commercial aluminum alloys, which enclose cell interior of low dislocation density. Such a dislocation network has significant influence on the hardening behavior and evolution of microstructure of the material during severe plastic deformation. Precipitations and dynamic precipitating also play important roles in thermomechanical processes of commercial aluminum alloys, which has to be taken into account in modeling of microstructure evolution of aluminum alloys.

The current multi-parameter dislocation model distinguishes the aforementioned two regions within the material. The spatial distribution of dislocations within each region is still treated as being homogeneous. This is due to the fact that the large number of dislocations do not allow an analytic treatment of individual dislocations. On the other hand, there is no simple analytical formula available which describes the evolution of the dislocation distribution during the deformation of dislocation network.

2.1 Kinetic equation of state

The 3IVM distinguishes three dislocation categories, namely, mobile dislocation(ρ_m), immobile dislocations in the cell interiors(ρ_i), and immobile dislocations in the cell walls(ρ_w). For each class of dislocations, an evolution law of the form will be derived:

$$\dot{\rho}_{m,i,w} = \dot{\rho}^{+}_{m,i,w} - \dot{\rho}^{-}_{m,i,w} \quad (1)$$

where $\dot{\rho}^{+}$ and $\dot{\rho}^{-}$ represent one or more production terms and reduction terms, respectively.

Within the 3IVM model, the Orowan equation is used as kinetic equation of state to calculate the applied stress of the material during thermomechanical process:

$$\dot{\gamma} = \dot{\varepsilon} \cdot M = \rho_m b v \quad (2)$$

where $\dot{\gamma}$ is the shear rate, M the Taylor factor of polycrystalline materials for the imposed strain path, and b the magnitude of the Burgers vector.

The average glide velocity of mobile dislocations v is calculated as

$$v = \lambda \upsilon_0 \exp\left(-\frac{Q}{k_B T}\right) \sinh\left(\frac{\tau_{eff} V}{k_B T}\right) \quad (3)$$

where λ is the jump width of dislocation, i.e. the mean spacing of obstacles (the immobile forest dislocation), υ_0 the attack frequency, Q the effective activation energy for dislocation glide, k_B Boltzman constant, V the activation volume, and T the deformation temperature. Then the effective shear stress τ_{eff} can be calculated by substituting Eqn. (3) into Eqn. (2).

As the forest dislocation spacing is different between the cell interiors and the cell walls, two different values for the effective stress, $\tau_{eff,i}$ in the cell interiors and $\tau_{eff,w}$ in the cell walls are obtained. The necessary resolved shear stress in the cell interior τ_i and in the cell walls τ_w can be derived as

$$\tau_{i(w)} = \tau_{eff,i(w)} + \alpha \dot{G} b \sqrt{\rho_{i(w)}} \quad (4)$$

where α is a constant and $\dot{G}$ the temperature dependent shear modulus.

The required external stress can then be calculated as

$$\sigma_{eff} = M(\varphi_i \tau_{eff,i} + \varphi_w \tau_{eff,w}) \quad (5)$$

where φ_i and φ_w are the volume fractions respectively. The Taylor factor for polycrystalline material can be calculated for arbitrary strain paths as a function of the total strain.

2.2 Mobile dislocation density

The mobile dislocations are assumed to penetrate through both dislocation walls and cell interiors. Each mobile dislocation is supposed to glide a mean free effective path F_{eff} before it is immobilized by one of the three processes described below. The externally imposed strain rate $\dot{\varepsilon}$ is found to have a relationship with the increscent rate of mobile dislocations $\dot{\rho}^{+}_m$ as

$$\dot{\varepsilon} = \dot{\rho}^{+}_m b F_{eff} \quad (6)$$

The mean effective path F_{eff} is determined by three obstacle spacing: the average free spacing of mobile dislocation in the cell walls F_w and in the interiors F_i, the grain size K and the distance between precipitates L_p as:

$$\frac{1}{F_{eff}} = \frac{\varphi_i}{F_i} + \frac{\varphi_w}{F_w} + \frac{1}{K} + \frac{1}{L_p} \quad (7)$$

The mobile dislocation density is decreased by three processes, namely the formation of dislocation dipoles, dislocation locks and dislocation annihilation. For each process a probability can be determined so that the reduction rates for the dislocation density are:

formation of dipoles:

$$\dot{\rho}^{-}_{m,d} = 2(d_d - d_{a-c}) \frac{\dot{\varepsilon} M}{b} \cdot \frac{1}{n} \cdot \rho_m \quad (8)$$

formation of locks:

$$\dot{\rho}_{m,l} = 4d_l \cdot \frac{\dot{\varepsilon}M}{b} \cdot \frac{n-1}{n} \cdot \rho_m \quad (9)$$

annihilation:

$$\dot{\rho}_{m,a-c} = 2d_{a-c} \cdot \frac{\dot{\varepsilon}M}{b} \cdot \frac{1}{n} \cdot \rho_m \quad (10)$$

where n is the number of active glide systems, and d_d, d_l, d_{a-c} the critical distances for the indicated processes, respectively.

2.3 Dislocation density in cell interiors

The increase of dislocation density inside the cells is equal to the decrease of mobile dislocations due to the formation of the locks:

$$\dot{\rho}_i^+ = \dot{\rho}_{m,l} = 4d_l \cdot \frac{\dot{\varepsilon}M}{b} \cdot \frac{n-1}{n} \cdot \rho_m \quad (11)$$

Since locks can not glide, the only process to decrease the immobile dislocation density is annihilation by dislocation climb. The rate equation for this process is given by

$$\dot{\rho}_i^- = 2v_c d_{a-g} \cdot \frac{1}{n} \cdot \rho_i^2 \quad (12)$$

where d_{a-g} is the critical distance of the two dislocations with antiparallel Burgers vectors when they are close enough to be annihilated along dislocation gliding direction, and v_c is the climb velocity controlled by thermal activation process.

v_c is calculated as

$$v_c = \tau A D / (k_B T)$$

where D is the diffusion coefficient, τ the shear stress and A the activation area.

2.4 Dislocation density in cell walls

The population of dislocations, named immobile dislocations in the cell walls ρ_m, undergo the same processes as those inside the cells, except that contributed to the increase of the dislocation density. To calculate the rate of increase of dislocations in the cell walls, the assumption that all dislocation dipoles accumulated in the cell walls should be taken into consideration. As dipoles are generated in the whole volume, but stored in the walls only, the rate of increased dislocations can be derived as

$$\dot{\rho}_w^+ = \frac{1}{\varphi_w}\dot{\rho}_{m,d} = \frac{2}{\varphi_w}(d_d - d_{a-c})\frac{\dot{\varepsilon}M}{b} \cdot \frac{1}{n} \cdot \rho_m \quad (13)$$

2.5 Precipitations

Concerning dislocation motions in heterogeneous commercial alloys, solid solution and precipitation hardening have to be taken into account. The non-deformable precipitations act as dislocation obstacles and affect the free spacing of the mobile dislocations both in the cell interiors and in the cell walls resulting from enhancement of dislocation glide resistance. On the other hand, the precipitations enlarge the activation energy for glide and lead to a larger glide resistance. Meanwhile, they also increase the yield stress by the Orowan stress:

$$\tau_O = \frac{Gb\sqrt{\varphi_p}}{r} \quad (14)$$

where φ_p is the volume fraction of precipitates and r the average precipitate radius. The ripening of precipitations during deformation at elevated temperatures cannot be neglected for it has effects on the precipitation radius, volume fraction and free spacing between neighboring precipitations. The increased hardening rate is taken by incorporating the precipitation spacing in the effective slip length:

$$L_p = \frac{r}{\sqrt{\varphi_p}} \quad (15)$$

For precipitate coarsening, the change of precipitate radius with time is given by

$$r = c(t + t_0)^{1/k} \quad (16)$$

where $k = 3$ for ideal Ostwald ripening.

The above equations are coupled and can be utilized to calculate the dislocation densities for each time step. One can calculate the evolution of three populations of dislocation density from Eqn. (6) to Eqn. (14). The external stress required to arrive at the imposed strain rate and at the given initial average dislocation density can be modeled by iteration from the Orowan equation, with the help of calculations of general dislocation density and the variation of effective shear stress in both cell interiors and cell walls. The stress—strain curves can then be derived out as a coupled constitutive equation in FEM simulation of thermomechanical process of the materials[5].

3 MODELLING OF HOT DEFORMATION OF Al-Mg-Si ALLOY

The physics based models require relevant data, which of most can economically obtained from physical simulation tests. In order to validate the current model, hot compression tests were performed at 450 and 500 ℃ with a constant strain rate of 0.001 s^{-1} on an Al-Mg-Si alloy (Al-0.62Mg-0.70Si-0.20Mn-0.03Cr). The experimental stress—strain curves were obtained from compression testing on Gleeble-1500 thermomechanical simulation machine. The experimental stress—strain curves of the Al-Mg-Si alloy exhibit a characteristic of peak stress at the beginning of deformation and subsequent smoothing in the imposed low strain rates and high temperatures, implying a less strain hardening than dynamic restoration[11], as shown in Fig. 1. This is caused by more thermal activation events and the possible ripening of precipitates in the matrix. During hot compression, dissolution of the precipitates leads to less precipitate vol-

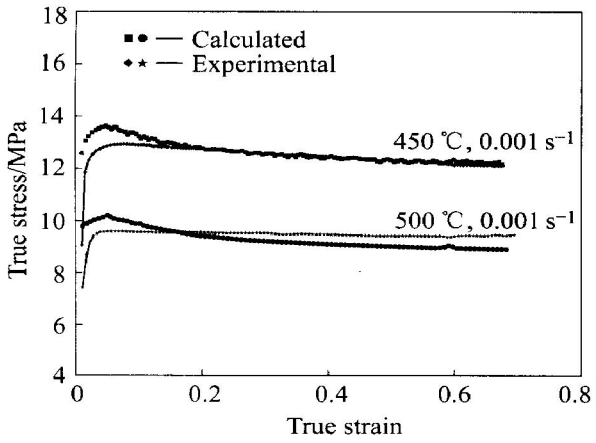

Fig. 1 Measured and computed stress—strain curves of Al-Mg-Si alloy

ume fraction and finer particle size.

The 3IVM was adopted in the hot compression of the alloy. The physical constants in above equations were set before the fitting process. Some material constants were chosen for pure aluminium[5, 6] and some special ones for the Al-Mg-Si alloy, as listed in Table 1. The volume fraction of cell interiors and cell walls were set to $\varphi_i = 0.9$ and $\varphi_w = 0.1$. The minimum distance for dislocation annihilation and climb, and the critical spacing for creation of dislocation locks are set to about 5 - 20 times of the magnitude of dislocation Burgers vector[6]. For a dipole to form, the distance between two dislocations has to exceed the critical distance for annihilation d_{a-c}, but has to be small enough to have the involved dislocations trap.

The remaining parameters were optimized by the means of random walk optimization algorithm within 10 000 iteration steps to obtain the lowest possible value for the mean square deviation of experimental and simulated stress—strain curves. The formation of textures during hot deformation is ignored in the modelling process. The optimized values are also outlined in Table 1, giving quite reasonable values of activation energies for commercial aluminium alloys[14, 15]. For the fitting process, the experimental data were used only up to a true strain of 0.7, because at larger strains the influence of friction became dominate, which was not accounted in the modelling. It can be seen from Fig. 1 that the computed stress—strain curves at different temperatures are in very good agreement with the experimental curves, where the mean deviation ratio is less than 5%.

Fig. 2 illustrates the evolution of the dislocation densities with the strain computed from the 3IVM model. The curves of the total (average) dislocation densities at different temperatures are quite similar to those of the experiment, implying

Table 1 Material parameters for 3IVM computation on Al-Mg-Si alloy

Constant	Given value	Optimized value
Elastic modulus[12] / GPa	69.0	
Shear modulus at 300 K / GPa	25.9	
Diffusion coefficient / ($m^2 \cdot s^{-1}$)	1.3×10^{-4}	
Initial grain size / m	1.0×10^{-4}	
Burgers vector of dislocation / m	2.86×10^{-10}	
Constant of diffusion (Mg in Al)[13] / ($m^2 \cdot s^{-1}$)	2.83×10^{-10}	
Constant of diffusion (Si in Al)[13] / ($m^2 \cdot s^{-1}$)	3.74×10^{-10}	
Taylor factor for polycrystalline materials	3.06	
Starting dislocation density at cell interior / m^{-2}	1.0×10^{6}	
Starting mobile dislocation density / m^{-2}	1.0×10^{9}	
Starting dislocation density at cell walls / m^{-2}	1.0×10^{9}	
Minimum distance in glide direction / m	$(1.0 - 5.0) \times 10^{-9}$	4.17×10^{-9}
Minimum distance for dislocation annihilation / m	$(1.0 - 5.0) \times 10^{-9}$	2.35×10^{-9}
Critical spacing for creation of dislocation locks / m	$(1.0 - 5.0) \times 10^{-9}$	2.71×10^{-9}
Constant for ripening	1.05×10^{-8}	
Activation energy for glide / eV	0.9 - 1.9	1.60
Activation energy for climb[14] / eV	1.45 - 1.62	1.47
Number of active glide systems	3 - 5	5
Volume fraction of precipitate	0.01 - 0.05	0.05
Attack frequency of dislocations / s^{-1}	$(6.8 - 7.8) \times 10^{9}$	7.14×10^{9}
Decrease of shear modulus with temperature / ($MPa \cdot K^{-1}$)	0.1 - 0.5	0.17

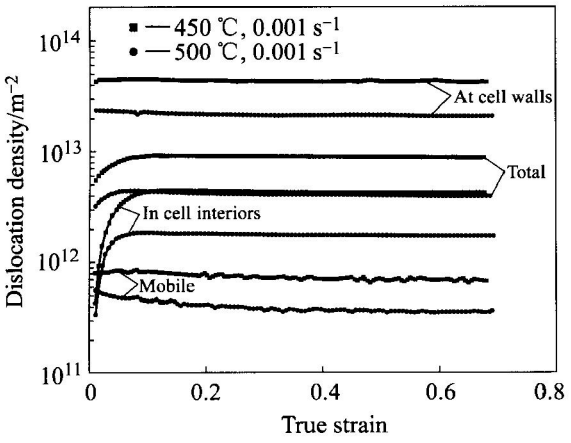

Fig. 2 Computed dislocation densities of Al-Mg-Si alloy at different temperatures

that the 3IVM has a very good computing accuracy. It is obvious that the change tendency of mobile dislocation is similar to that of average dislocation density, with a maximum value around true strain of 0.05, which is consistent to the stress—strain curves as shown in Fig. 1. Nevertheless, the densities of both the mobile dislocations and dislocations in the cell walls possess the characteristic of maximum value at the beginning of deformation and becoming smooth with increase of strain. Such a decrease can be resulted from the dislocation interactions, concomitant formation of dislocation dipoles and dislocation locks in the cell interiors with the exhaustion of mobile dislocations.

The dislocation density in the cell interiors is about 90% of that at the cell walls, which is consistent to the correspondent volume fractions of the cell interiors and the cells walls in the material. The mobile dislocation density is only about 5.8% of the total dislocation density at lower temperature, while at higher temperature more than 7% of the total dislocations are mobile dislocations. Dislocation density decreases with the increase of deformation temperature due to more dislocation climb and thermal activation sites at higher temperatures with the help of imposed external stress for the alloy.

Acknowledgements

The authors wish to express their acknowledge to Southwest Aluminium Fabrication Plant for supplying the material. One of the authors, SHEN Jian, is grateful to Dipl. M. Goerdeler for his assistance during Shen's stay at IMM.

REFERENCES

[1] Li Y Y. Summary on material science and engineering development[A]. Symposium of the 81st Xiangshan Academic Conference on Science[C]. Xiangshan, Beijing: 1997. 9-11.

[2] Zhu Q, Sellars C M. Microstructural evolution of aluminium-magnesium alloys during thermomechanical processing[J]. Materials Science Forum, 2000, 331-337: 409-420.

[3] Marthinsen K, Nes E. The ALFLOW-model: A microstructureal approach to constitutive plasticity-modelling of aluminium alloys[J]. Materials Science Forum, 2000, 331-337: 1231-1242.

[4] Brand A J, Kalz S, Henningsen P, et al. 3D-simulation of closed pass rolling with intergrated microstructural simulation[A]. Beynon J H, Ingham P, et al. Proc. of the 2nd Inter. Conf. on Modeling of Metal Rolling Processes [C]. London, UK: 1996. 2-11.

[5] Roters F. Realization of Multiplane Concept in the Plasticity Modeling—From the Dislocation Dynamics to the Finite Element Simulation[D]. RWTH-Aachen, Germany. 1998.

[6] Roters F, Raabe D, Gottstein G. Calculation of stress-strain curves by using 2 dimensional dislocation dynamics [J]. Computational Materials Science, 1996, 7: 56-62.

[7] Lagneborg R, Zajac S, Hutchinson B. A model for the flow stress bahaviour during hot working of aluminium alloys containing non-deformable precipitates[J]. Scripta Metallurgica et Materialia, 1993, 29: 159-164

[8] Seefeldt M, Klimanek P. Modelling of microstructure development by means of a dislocation-dislocation reaction kinetics[J]. Computational Materials Science, 1997, 9: 267-273.

[9] Sellars C M. Modelling microstructural development during hot rolling[J]. Materials Science and Technology, 1990, 6(11): 1072-1081.

[10] Roters F, Raabe D, Gottstein G. Work hardening in heterogeneous alloys—a microstuctural approach based on three internal state variables[J]. Acta Materia, 2000, 48: 4181-4190.

[11] Shen J, Goerdeler M, Gottstein G. Recrystallization and grain growth[A]. Gottstein G, Molodov D A. Proc. of the First Joint International Conference[C]. Springer-Verlag Berlin Heidelburg, New York: 2001. 1317-132.

[12] Mondo Ifo L F. Aluminium Alloys: Structure and Properties[M]. New York: The Butterworths Group, 1976. 66-67.

[13] Smithells C J. Metals Reference Book, 3rd Edition, Volume 2[M]. Berlin: Pergamon Press, 1962. 598-599.

[14] Rao K P, Prasad Y V R K. High temperature deformation kinetics of Al-4Mg alloy[J]. Journal of Mechanical Working Technology, 1986, 13: 83-95.

[15] Poirier J P. Guan De-lin tr. High-temperature Plastic Deformation of Crystals[M]. Dalian: Dalian University of Technology Press, 1989. 24-50.

(Edited by YANG Bing)